Internal Wave Spectra at the Buoyant and Inertial Frequencies

WALTER H. MUNK

Scripps Institution of Oceanography, University of California, San Diego, La Jolla 92093

(Manuscript received 22 April 1980, in final form 23 July 1980)

ABSTRACT

Spectra of the vertical displacement (potential energy) have been observed to be only slightly enhanced at the buoyancy frequency $\omega = N$, whereas spectra of horizontal velocity u, v (kinetic energy) are greatly enhanced at the inertial frequency $\omega = f$ (except at equatorial latitudes). Consequently, the former are ignored in certain model spectra, whereas the latter are allowed for explicitly [e.g., by a term $(\omega^2 - f^2)^{\mp 1/2}$). I have attempted to interpret these observations in terms of the behavior of free wave packets at the turning points. *Local* resonant generation may also be a factor (Fu, 1980) but is not considered here.

In this tutorial $N' = dN/dz$ and $f' = df/dy \equiv \beta$ are taken as constant in order to make the derivation of the solutions near N and f as simple and as parallel as possible; these turning point solutions (in terms of Airy functions) fail in narrow waveguides, e.g., near a sharp buoyancy peak and at equatorial latitudes. The β-plane approximation fails at polar latitudes. Limit functions are evaluated numerically for a superposition of wave modes with relative energy $(j^2 + j_*^2)^{-1}$, $j = 1, 2 \ldots, j_* = 3$, assuming horizontal isotropy. The computed cutoffs are smooth functions of frequency, with a peak just below N and just above f, respectively. The N amplification in the vertical displacement spectrum is by less than 2 (but equals 5 for the spectrum of vertical strain rate). The f amplification in the horizontal velocity spectrum is by a factor of 8 at latitude $\theta = 30°$, and diminishes with latitude as $(\sin\theta \tan\theta)^{1/3}$. In general, the amplification varies with the width of the waveguide (vertical and latitudinal) expressed in units of a characteristic wavelength. Thus the inertial peak is a consequence of linear wave theory and should not be independently imposed on model spectra.

1. Introduction

Why is the inertial (or Coriolis) peak so prominent in the spectra of horizontal motion in the sea, whereas the buoyancy (or Brunt-Väisälä) peak is a minor feature in the spectra of vertical motion? The mathematical structure for the two cases is very similar, yet there are differences and these differences do account for some of the observational features.

The following derivation follows the classical WKB treatment of free waves at turning points. The derivation of the differential equations for the wave functions $W(z)$ and $V(y)$ is quite standard. I then give the uniformly valid solution for the N cutoff (derived by Desaubies 1972, 1975). The analogous solution for the f cutoff is obtained from a generalization of Munk and Phillips (1968). In the appropriate Airy scales, the vertical waveguide $[N(z) \geqslant \omega]$ measures just a few units, whereas the equatorial waveguide $[f \leqslant \omega]$ measures many such units, and this is related to the relative prominence of the inertial peak.

In this tutorial $N' = dN/dz$ and $f' = df/dy \equiv \beta$ are taken as constant in order to make the solutions near N and f as simple and as similar as possible. These isolated turning point solutions (in terms of Airy functions) fail for narrow waveguides, whether vertical or latitudinal. Eriksen (1978, 1980) has given the solution for two turning points in terms of Hermite polynomials, and these are appropriate at low latitudes. At high latitude the β approximation fails. Fu (1980) uses the globally valid solutions in terms of spheroidal wave functions—at the expense of losing some of the analytical transparency of the simple asymptotic formulation.

We are concerned entirely with turning point enhancement of waves generated at lower latitudes; there is also a resonance enhancement of locally generated waves (Fu, 1980).[1]

Let $F(\omega,j,\alpha)$ designate an internal wave spectrum as a function of frequency, vertical modenumber and azimuth angle, well away from both turning points. The frequency spectrum is written

$$F(\omega) = \sum_j \int_\alpha d\alpha F(\omega,j,\alpha), \quad f \ll \omega \ll N.$$

A simple spectrum that allows for the f and N cutoffs is

[1] C. Garrett has made the interesting suggestion that one should be able to separate experimentally the remote and local generations of inertial waves. For remote generation, waves moving toward and away from the turning latitude should become increasingly phase-locked with proximity to the turning point.

0022-3670/80/111718-11$06.75

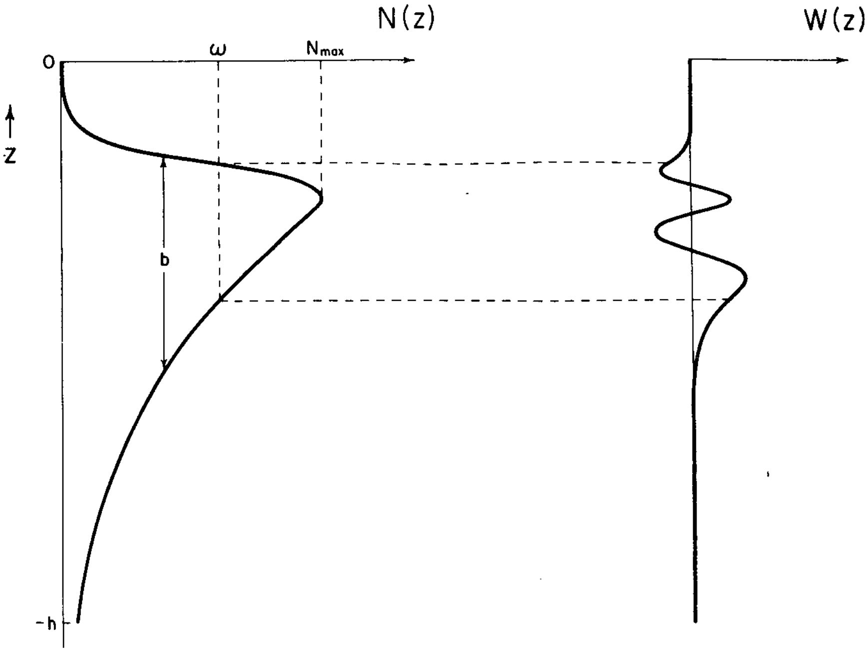

FIG. 1. Depth variation of the buoyancy frequency $N(z)$ showing a maximum N_{max} at the thermocline. b is a stratification scale, which can be related to the overall dimension to the N peak, or at greater depth to the logarithmic decrement of $N(z)$: $b^{-1} = N^{-1}\, dN/dz$. The wave function $W(z)$ is drawn for a fixed ω, and for mode number $j = 4$.

$$H(\omega - f)H(N - \omega)F(\omega),$$

where H is the stepfunction. Garrett and Munk (1972) proposed a spectrum of the form

$$\omega(\omega^2 - f^2)^{-1/2}H(\omega - f)H(N - \omega)F(\omega)$$

to allow for the observed spectral peak at $\omega = f$. Here I shall use the formalism

$$I_f(\omega - f)I_N(N - \omega)F(\omega).$$

The limiting functions $I(x)$ have similar asymptotic behaviors as the stepfunction $H(x)$; they are to be derived assuming that the mode weighting and directional distribution are the same at the turning points as they are for the spectrum $F(\omega,\alpha,j)$ away from the turning points.

2. Boussinesq equations[2]

We start with the usual Boussinesq equations

$$\partial_t u - fv = -\partial_x p, \quad (1)$$

$$\partial_t v + fu = -\partial_y p, \quad (2)$$

$$\partial_t w - b = -\partial_z p, \quad (3)$$

$$\partial_t b + N^2 w = 0, \quad (4)$$

$$\partial_x u + \partial_y v + \partial_z w = 0, \quad (5)$$

where $b = g(\rho_0 - \rho)/\rho_0$ is the buoyancy, and p the perturbation pressure divided by ρ_0. Otherwise the notation is standard.

Eqs. (3) and (4) are combined into

$$\partial_{tt} w + N^2 w = -\partial_{zt} p, \quad (6)$$

leaving four equations in four unknowns. The solutions are written as east-going progressive waves:

$$\begin{bmatrix} u \\ v \\ w \\ p \end{bmatrix} = e^{i(kx-\omega t)} \begin{bmatrix} UZ \\ iVZ \\ iPW \\ cPZ \end{bmatrix}, \quad (7)$$

where U, V, P are functions of y (north), and W, Z are functions of z (up); c is an undetermined parameter with dimensions of velocity.

A substitution of (7) into (5) can be put in the form

$$\frac{kU + V'}{P} = -\frac{W'}{Z} = \frac{\omega}{c}, \quad (8)$$

where $V' = dV/dy$ and $W' = dW/dz$. The first term is a function only of y, the second term only of z. We can then equate both sides to a separation parameter which does not depend on y or z, which we call ω/c. $W' = -(\omega/c)Z$, which is combined with (6) to give

$$W'' + m^2 W = 0, \quad m^2 = c^{-2}(N^2 - \omega^2). \quad (9)$$

[2] The reader may wish to go at once to Section 3.

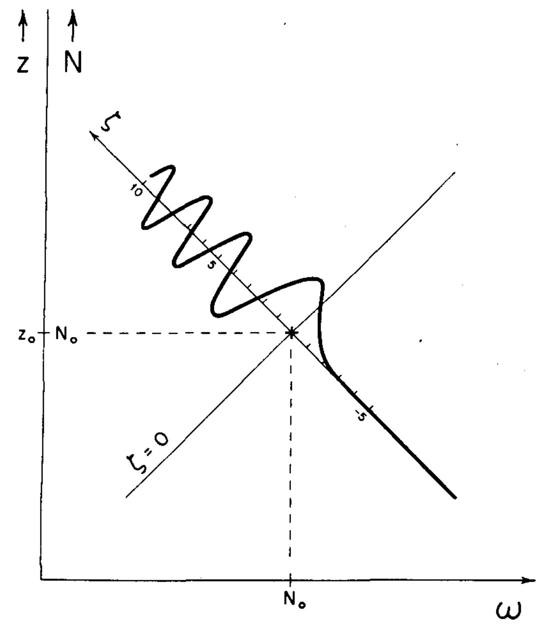

FIG. 2. The Airy finestructure near the *lower* turning point (beneath the N maximum). z is upward from the surface (z_0 is negative). The z axis is labeled in terms of the corresponding values of the buoyancy frequency $N(z)$. ζ is positive upward (downward at the *upper* turning point). The line $\zeta = 0$ is drawn, and $\mathrm{Ai}(-\zeta)$ is sketched relative to the slanted ζ axis. Turning depths are along $\zeta = 0$.

The first term of (8) is now equated to the separation parameter:

$$kU + V' = (\omega/c)P, \tag{10}$$

which, together with the results from the remaining equations [(1) and (2)],

$$\omega U + fV = kcP, \tag{11}$$

$$\omega V + fU = -cP', \tag{12}$$

gives three equations [(10), (11), (12)] in the three unknowns U, V, P. These are combined into

$$V'' + l^2 V = 0, \quad l^2 = c^{-2}(\omega^2 - f^2) - k^2 - \beta k/\omega, \tag{13}$$

with $\beta = df/dy$. This is the usual β-plane formulation. Notice from (13) and (9) that

$$\kappa^2 \equiv k^2 + l^2$$

$$= \frac{\omega^2 - f^2}{c^2} - \frac{\beta k}{\omega} = m^2 \frac{\omega^2 - f^2}{N^2 - \omega^2} - \frac{\beta k}{\omega}. \tag{14}$$

For the f-plane solution, e.g., $\beta = 0$, this gives the usual expression for the slope m/κ of the wave propagation vectors as a function of ω. Further, one obtains from (9)

$$\frac{\omega^2}{\kappa^2} = \frac{c^2}{1 - f^2/\omega^2},$$

so that we identify the separation constant c with the horizontal phase velocity ω/κ away from the inertial frequency (where phase velocity goes to infinity and group velocity goes to zero).

3. Wave solution at the buoyancy frequency

The simplest case is that of an isolated N-peak imbedded in an infinitely deep ocean. Within a waveguide, determined by $\omega < N$, $W(z)$ is trigonometric; outside the waveguide, $\omega > N$, the wave function decays exponentially. The transition occurs at the *turning depths*. The condition for trapping within the guide imposes certain restraints on $m(z)$. In a WKBJ treatment this leads to

$$m(\omega, j;\, z) = \frac{j\pi}{b}\left(\frac{N^2(z) - \omega^2}{N_{\max}^2 - \omega^2}\right)^{1/2},$$

$$j = 1, 2, \ldots, \tag{15}$$

for waveguides as sketched in Fig. 1, provided b is suitably related to the vertical extent of the $N(z)$ peak.[3] In the case of surface and bottom boundaries at $z = 0$ and $z = -h$, Eq. (15) is still applicable beneath the thermocline provided $|h| \gg b$, and b is defined by the e-folding scale of $N(z)$: $b^{-1} = \rho^{-1}d\rho/dz$. A typical value is $b = 1$ km. The separation parameter is found from (9) and (15):

$$c_j = \frac{b}{j\pi}(N_{\max}^2 - \omega^2)^{1/2} \approx \frac{bN_{\max}}{j\pi}. \tag{16}$$

(The approximation is adequate since we shall stay away from the N peak.)

From Eqs. (9), (15) and (16) we have

$$\partial_{zz} W + m^2 W = 0,$$

$$m^2(\omega, j;\, z) = c_j^{-2}[N^2(z) - \omega^2], \tag{17}$$

for $\omega \ll N_{\max}$. A uniformly valid solution is given by Desaubies (1972, 1975):

$$W = m^{-1/2}\zeta^{1/4}\,\mathrm{Ai}(-\zeta), \quad \zeta = \left[\frac{3}{2}\int_{z_1}^{z} m dz\right]^{2/3}. \tag{18}$$

Consider the situation in the neighborhood of a reference level z_0 (Fig. 2). We wish to explore the internal wave behavior near z_0, and at frequencies close to

$$\omega_0 = N(z_0) \equiv N_0. \tag{19}$$

The value of m at the reference point is zero:[4]

$$m_0 \equiv m(\omega_0, j;\, z_0) = 0. \tag{20}$$

---

[3] $\int_{-h}^{0} dz(N^2 - \omega^2)^{1/2} = b(N_{\max}^2 - \omega^2)^{1/2}$. In the precise formulation j should be replaced by $j - ½$.

[4] The notation is more elaborate than here required, in order to prepare for a parallel notation for the inertial frequency.

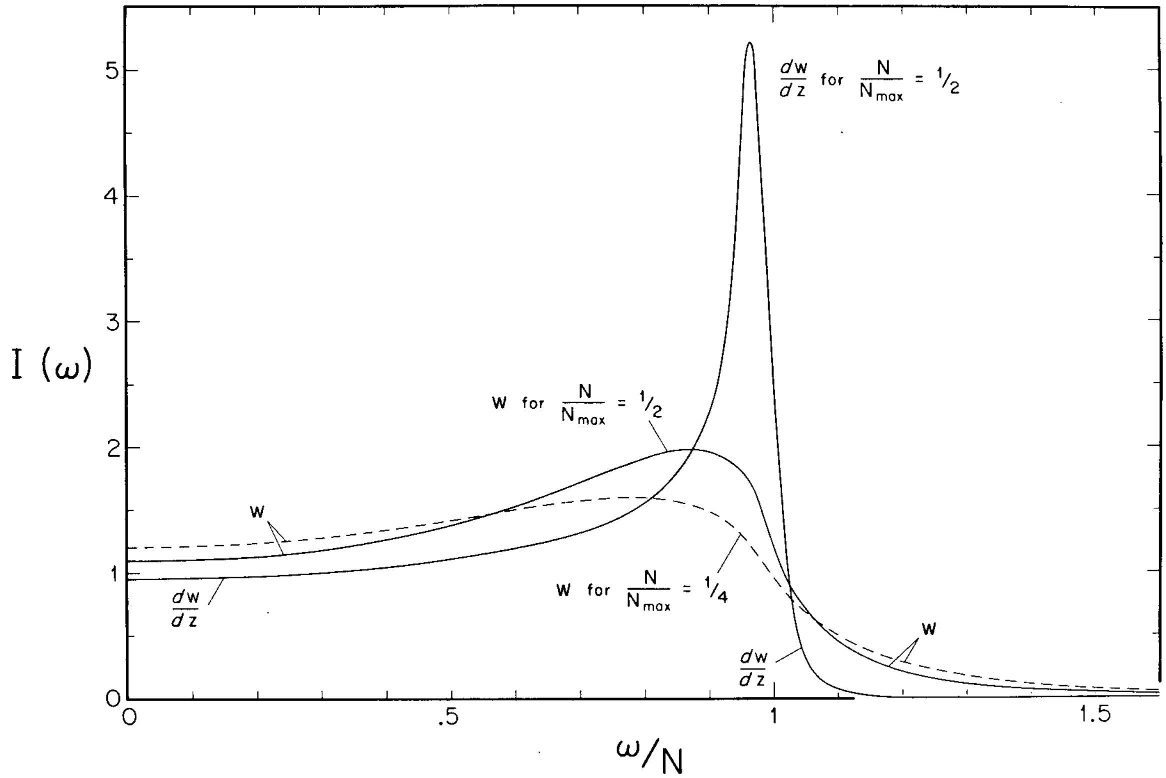

FIG. 3. The mode-weighted buoyancy limit function $I(\omega)$ for the spectrum of the vertical velocity w (or the vertical displacement $\int w dt$) for a shallow ($N = \frac{1}{2}N_{max}$) and deep ($N = \frac{1}{4}N_{max}$, dashed) turning depth; and for vertical strain rate dw/dz at $N = \frac{1}{2}N_{max}$. The mode weighting for w is by $(j^2 + j^{*2})^{-1}$ with $j^* = 3$; for dw/dz it is approximated by $j^2(j^2 + j^{*2})^{-1}$ with an upper limit $j = 100$.

We take any frequency ω near ω_0 and define $z_1(\omega)$ by the condition that it is a turning depth, i.e.,

$$m_1 \equiv m(\omega,j;\, z_1) = 0, \tag{21}$$

so that

$$N(z_1) \equiv N_1 = \omega. \tag{22}$$

In the near field,

$$N^2 - N_1^2 \approx 2N_0 N'(z - z_1). \tag{23}$$

This involves two separate assumptions: $N + N_1 \approx 2N_0$ and $N - N_1 \approx N'(z - z_1)$. (In our example we shall assume that the second condition applies exactly and indefinitely.) Within the near field, the solution (18) reduces to

$$W = z_A^{1/2}\,\mathrm{Ai}(-\zeta), \quad \zeta = \frac{z - z_1}{z_A},$$

$$z_A{}^3 = \frac{c_j}{2N'N_0}, \quad |\zeta| \ll 1.$$

But well above the lower turning depth we have $N^2 \gg \omega^2$, and the asymptotic form of the uniformly valid solution is

$$W = \pi^{-1/2} z_A{}^{1/2} \zeta^{-1/4} \sin[(\tfrac{2}{3}\zeta)^{3/2} + \tfrac{1}{4}\pi]$$
$$= \pi^{-1/2} c_j{}^{1/2} N^{-1/2}(z) \sin[(\tfrac{2}{3}\zeta)^{3/2} + \tfrac{1}{4}\pi],$$
$$\zeta \gg 1, \tag{24}$$

so that W varies as $N^{-1/2}$ in accordance with the usual WKB approximation.

4. Buoyancy limit function

The asymptotic value of W^2 averaged over many wiggles is

$$\langle W^2 \rangle = \tfrac{1}{2}\pi^{-1} N^{-1} c_j.$$

Accordingly, we define the normalized limit function

$$G(\omega,j;\, z) = 2\pi N c_j{}^{-1} W^2 = 2\pi N c_j{}^{-1} m^{-1} \zeta^{1/2}\,\mathrm{Ai}^2(-\zeta), \tag{25}$$

$$\zeta^{3/2} = \frac{3}{2}\int_{z_1}^{z} m dz, \quad m^2 = c_j{}^{-2}[N^2(z) - \omega^2], \tag{26}$$

with z_1 defined by $m(\omega,j;\, z_1) = 0$. Hence $\langle G \rangle \to 1$ for large $+\zeta$ and $\langle G \rangle \to 0$ for large $-\zeta$.

We now specialize to the case of constant $N' = dN/dz$. Replacing dz by dN/N' in (26) yields

$$\zeta^{3/2} = \tfrac{3}{2} c_j^{-1}(N')^{-1} \int_{N_1}^{N} (N^2 - \omega^2)^{1/2} dN, \quad N_1 = \omega,$$

$$= \tfrac{3}{4} c_j^{-1}(N')^{-1}\omega^2 \left\{ \frac{N}{\omega}\left(\frac{N^2}{\omega^2} - 1\right)^{1/2} - \ln\left[\frac{N}{\omega} + \left(\frac{N^2}{\omega^2} - 1\right)^{1/2}\right] \right\}$$

$$= jK_N{}^3 \phi^3(\mu), \quad \omega = N \cos\mu; \tag{27}$$

with

$$K_N{}^3 = \frac{\pi N^2}{2bN'N_{\max}} \approx \frac{\pi}{2}\frac{N}{N_{\max}} \tag{28}$$

and

$$\phi^3(\mu) = \tfrac{3}{2}[\sin\mu - \cos^2\mu \ln\tan(\tfrac{1}{2}\mu + \tfrac{1}{4}\pi)] = \sin^3\mu + \cdots. \tag{29}$$

The ratio $\phi/\sin\mu$ is nearly constant, varying from 1 to 1.15 as μ goes from 0 to 90°.

Similarly for $\omega \geqslant N$,

$$\zeta^{3/2} = -jK_N{}^3\psi^3(\nu), \quad \omega = N \sec\nu, \tag{30}$$

$$\psi^3(\nu) = \tfrac{3}{2}(\nu \sec^2\nu - \tan\nu) = \tan^3\nu + \cdots. \tag{31}$$

From (25)

$$\langle G(\omega,j)\rangle$$

$$= 2\pi K_N \frac{\phi}{\sin\mu} j^{1/3} \langle \mathrm{Ai}^2(-\zeta)\rangle \to \csc\mu, \quad +\zeta \gg 1,$$

$$= 2\pi K_N \frac{\psi}{\tan\nu} j^{1/3}\, \mathrm{Ai}^2(-\zeta) \to \frac{\exp - [\tfrac{4}{3}(-\zeta)^{3/2}]}{2\tan\nu}, \quad -\zeta \gg 1,$$

for $\omega \leqslant N$ and $\omega \geqslant N$, respectively. Finally, at the turning point $\omega = N$, $\zeta = 0$, and

$$G(\omega,j) = 2\pi K_N j^{1/3}\, \mathrm{Ai}^2(0).$$

5. Mode weighting for buoyancy limit

The summed limit function from a superposition of j modes, each weighted according to $H(j)$, is

$$I(\omega) = \sum_j H(j)G(\omega,j), \quad \sum_j H(j) = 1. \tag{32}$$

The role of j enters through $\zeta \approx j^{2/3}$. The smearing associated with cutoff can now be visualized, each mode being characterized by an appropriate *stretching* of the frequency scale, but all modes being secured to the inflection point at $\zeta = 0$, $\omega = N$. (In the case of the inertial peak there will be further smearing associated with the *shifting* of the inflection point according to the value of the east-west wavenumber k.)

Fig. 3 shows the limit function with mode-weighting according to the GM spectrum (Garrett and Munk, 1972; Munk, 1980):

$$H(j) = J(j^2 + j_*{}^2)^{-1}. \tag{33}$$

Here $j_* = 3$ is a scale mode number; $J = 2.18$ is determined by

$$\sum_{j=1}^{\infty} H(j) = 1.$$

Maximum amplification of the w spectrum is by a factor 2 at a depth where $N = \tfrac{1}{2}N_{\max}$ (typically 700 m depth) and even less for $N = \tfrac{1}{4}N_{\max}$ (1400 m).

The amplification is relatively small because of the j^{-2} suppression of the higher modes in the spectrum of vertical velocity w (or equivalently the vertical displacement $\int w dt$). The amplification is also shown for a (normalized) mode-weighting $j^2H(j)$ between $j = 1$ and $j = 100$, corresponding roughly[5] to the situation for vertical strain rate dw/dz. Here the amplification is much larger because of the enhanced role played by the high vertical wavenumbers.

6. Wave solution at the inertial frequency

This will parallel the preceding development. From (13)

$$\partial_{yy}V + l^2V = 0,$$

$$l^2(\omega,j,k;y) = c_j^{-2}(\omega^2 - f^2) - k^2 - \beta k/\omega. \tag{34}$$

A uniformly valid solution is

$$V = l^{-1/2}(-\eta)^{1/4}\,\mathrm{Ai}(\eta), \quad -\eta = \left(\frac{3}{2}\int_y^{y_1} l dy\right)^{2/3}. \tag{35}$$

Consider the situation in the neighborhood of a reference latitude ϕ_0, with corresponding inertial frequency $f_0 = 2\Omega \sin\phi_0$ (Fig. 4). The distance y is positive northward, and $a(\phi - \phi_0) = y - y_0$, with a the earth's radius. We are concerned with frequencies in the neighborhood of

$$\omega_0 = f(y_0) \equiv f_0. \tag{36}$$

The value of l at the reference point is given by

$$l_0{}^2 \equiv l^2(\omega_0,j;y_0) = -k^2 - \beta k/\omega_0, \tag{37}$$

and is not generally zero (unlike m_0) except at $k = 0$. We take any elementary wave train (ω,j,k), and define $y_1(\omega,j,k)$ by the turning condition

$$l_1 \equiv l(\omega,j,k;y_1) = 0, \tag{38}$$

so that

$$f_1{}^2(\omega,j,k) = \omega^2 - c_j{}^2(k^2 + \beta k/\omega). \tag{39}$$

It can be shown (the Appendix) that the term $\beta k/\omega$ can be neglected since $k^2{:}\beta k/\omega$ is of order ka (the number of wavelengths around the earth's circumference), and thus very large.

In the near-field approximation,

[5] The exact procedure involves the differentiation of the Airy function. This has not been done.

$$V = y_A^{1/2}\,\mathrm{Ai}(\eta), \quad \eta = \frac{y - y_1}{y_A},$$

$$y_A^3 = \frac{c_j^2}{2\beta f_0}, \quad |\eta| \ll 1.$$

But well toward the equator we have $f^2 \ll \omega^2$, and the asymptotic form of the uniformly valid solution is

$$\begin{aligned} V &= \pi^{-1/2} y_A^{1/2}(-\eta)^{-1/4} \sin[(-\tfrac{2}{3}\eta)^{3/2} + \tfrac{1}{4}\pi] \\ &= \pi^{-1/2}(c_j^{-2}\omega^2 - k^2)^{-1/4} \sin[(-\tfrac{2}{3}\eta)^{3/2} + \tfrac{1}{4}\pi], \\ &\qquad -\eta \gg 1, \end{aligned} \tag{40}$$

so that the amplitude of V is independent of y. [In the corresponding asymptotic expression (24), the amplitude of W is proportional to $N^{-1/2}(z)$. The difference arises essentially from the fact that the waveguides are associated with a f minimum and a N maximum, respectively.]

7. Inertial limit function for $\omega > f$

On the equatorial (oscillatory) side of the turning latitude, l^2 is positive and η negative. The value of V^2 averaged over many wiggles is

$$\langle V^2 \rangle = \tfrac{1}{2}\pi^{-1}(c_j^{-2}\omega^2 - k^2)^{-1/2}.$$

Accordingly, we define the normalized limit function

$$\begin{aligned} G(\omega,j,k;y) &= 2\pi(c_j^{-2}\omega^2 - k^2)^{1/2}V^2 \\ &= 2\pi[c_j^{-2}\omega^2 - k^2]^{1/2} l^{-1}(-\eta)^{1/2}\,\mathrm{Ai}^2(\eta), \end{aligned} \tag{41}$$

$$(-\eta)^{3/2} = \frac{3}{2}\int_y^{y_1} l\,dy, \quad l^2 = c_j^{-2}[\omega^2 - f^2(y)] - k^2, \tag{42}$$

with y_1 defined by $l(\omega,j,k;y_1) = 0$. Hence $\langle G \rangle \to 1$ for large $-\eta$ and $\langle G \rangle \to 0$ for large $+\eta$.

We now specialize to the case of a constant $\beta = df/dy$. A convenient notation is

$$\sigma^2 = \omega^2 - c_j^2 k^2, \quad l^2 = c_j^{-2}(\sigma^2 - f^2). \tag{43}$$

Thus

$$\begin{aligned} (-\eta)^{3/2} &= \tfrac{3}{2} c_j^{-1}\beta^{-1}\int_f^{f_1} (\sigma^2 - f^2)^{1/2} df, \quad f_1 = \sigma \\ &= \tfrac{3}{4} c_j^{-1}\beta^{-1} f^2(\gamma \sec^2\gamma - \tan\gamma), \\ &\cos\gamma = f/\sigma. \end{aligned}$$

Finally, we need to allow for the directional dependence of the internal wave spectrum. Set

$$k = \kappa\cos\alpha, \quad l = \kappa\sin\alpha, \quad \kappa = c_j^{-1}(\omega^2 - f^2)^{1/2}. \tag{44}$$

Then with $k = c_j^{-1}(\omega^2 - f^2)^{1/2}\cos\alpha$, one finds from (43) that

$$\begin{aligned} \sigma^2 &= \omega^2\sin^2\alpha + f^2\cos^2\alpha, \\ (-\eta)^{3/2} &= jK_f^3\psi^3(\gamma), \quad \tan\gamma = \sin\alpha\tan\nu, \\ \omega &= f\sec\nu, \end{aligned} \tag{45}$$

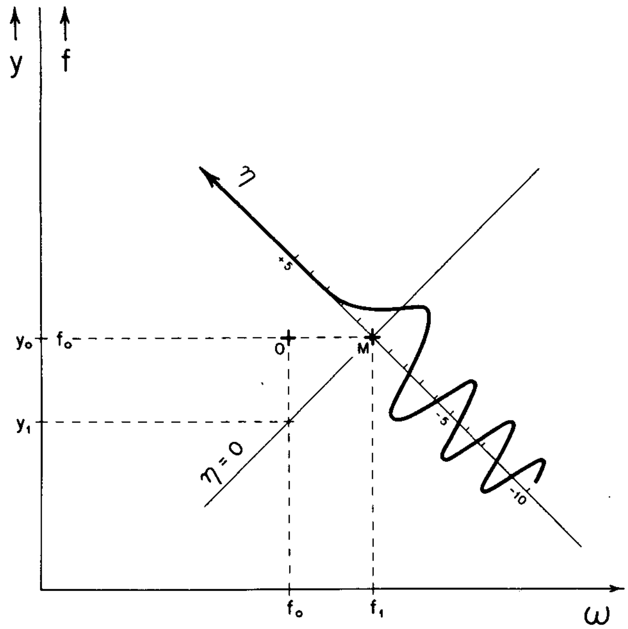

FIG. 4. The Airy finestructure in the turning latitudes north of the equator. The y axis (positive northward) is labeled in terms of the corresponding value of the inertial frequency $f(y)$. η is positive northward (southward in the Southern Hemisphere). The line $\eta = 0$ is drawn, and $\mathrm{Ai}(+\eta)$ is sketched relative to the slanted η axis. Turning latitudes are along $\eta = 0$. The distance $\mathrm{OM} = \beta k^2 y_A^3$ is the "blueshift" of the turning frequency relative to the local inertial frequency.

$$\begin{aligned} K_f &= \left(\frac{\pi f^2}{2b\beta N_{\max}}\right)^{1/3} = K_0(\sin\theta\,\tan\theta)^{1/3}, \\ K_0 &= \left(\frac{\pi a\Omega}{bN_{\max}}\right)^{1/3} = 6.53, \end{aligned} \tag{46}$$

$$\psi^3(\gamma) = \tfrac{3}{2}(\gamma\sec^2\gamma - \tan\gamma) = \tan^3\gamma + \cdots,$$

where θ is latitude and a, Ω are the earth's radius and angular velocity. From (41)

$$\langle G(\omega,j,\alpha)\rangle = 2\pi K_f(\psi/\sin\gamma) j^{1/3}\langle \mathrm{Ai}^2(\eta)\rangle \to \csc\gamma$$

for

$$-\eta \gg 1. \tag{47}$$

We now make the assumption that the spectrum in the equatorial waveguide ($\omega > f$) is horizontally isotropic. This is the simplest case, and the one selected in the GM model. There is some evidence for isotropy well above the inertial frequency, but I know of no evidence for isotropy at the turning point. The weighted limit function is

$$I(\omega) = \sum_j H(j)\,\frac{2}{\pi}\int_0^{\pi/2} d\alpha\, G(\omega,j,\alpha). \tag{48}$$

Anisotropy away from the turning latitudes could be allowed for by some function $A(\alpha)$ in Eq. (48).

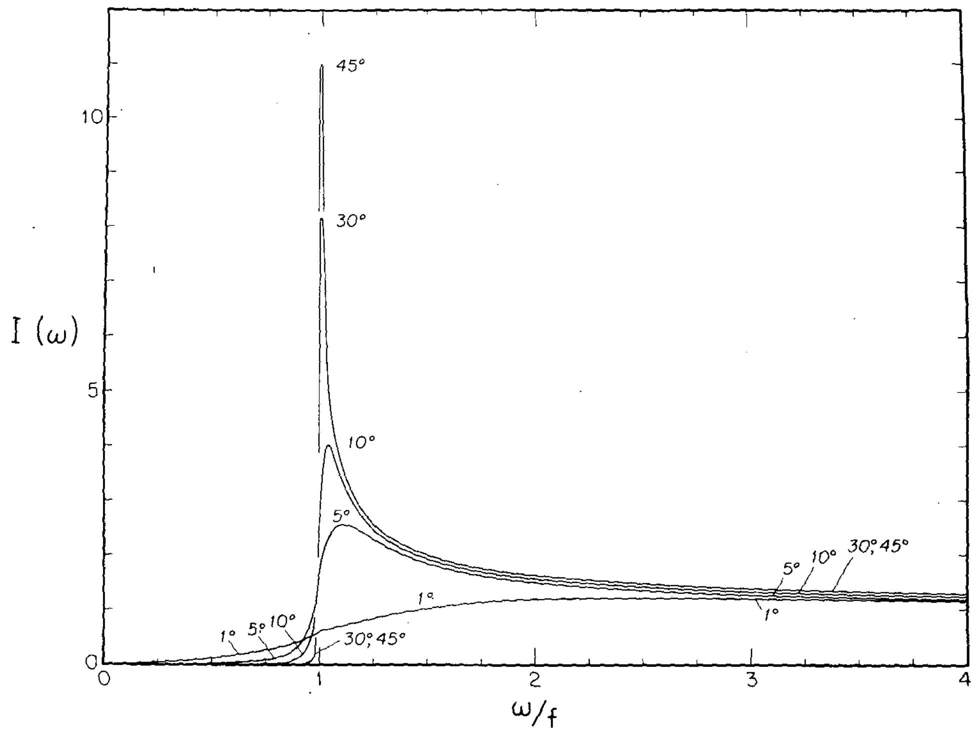

FIG. 5. The mode-weighted limit function $I(\omega)$ for the spectrum of velocity v at latitudes 1°, 5°, 10°, 30°, 45°. Mode weighting is by $(j^2 + j_*^2)^{-1}$, with $j_* = 3$.

8. Inertial limit function for $\omega < f$

The simplest continuation into the sub-inertial frequencies is to leave $k = 0$ for $\omega < f$. This then corresponds to isotropic generation within the waveguide, and WKB leakage (but no generation) beyond the waveguide.

With $k = 0$,

$$\eta^{3/2} = \tfrac{3}{2} c_j^{-1} \beta^{-1} \int_{f_1}^{f} (f^2 - \omega^2)^{1/2} df, \quad f_1 = \omega, \tag{49}$$

$$= jK_f^3 \phi^3(\mu), \quad \omega = f \cos\mu$$

$$G(\omega,j) = 2\pi K_f(\phi/\tan\mu) j^{1/3}\,\mathrm{Ai}^2(\eta),$$

$$I(\omega) = \sum_j H(j)G(\omega,j), \tag{50}$$

with $\phi(\mu)$ defined in Eq. (29).

The weighted limit functions $I(\omega)$ at selected latitudes are plotted for v and $v' = dv/dz$ in Figs. 5 and 6. The v' peak exceeds the v peak, as was the case for w' versus w. (I know of no reason why one should want dv/dz.) The v peak disappears at equatorial latitudes.

9. Airy scales

Collecting formulas, we have the following Airy scales:

Buoyancy depth scale	$z_A \doteq 2^{-1/3}\left[\dfrac{N_{\max}}{j\pi N_0}\right]^{2/3} b$	0.28 km
Buoyancy frequency scale	$N' z_A = 2^{-1/3}\left[\dfrac{N_{\max}}{j\pi N_0}\right]^{2/3} N_0$	0.74×10^{-3} s^{-1} (0.42 cph)
Inertial north scale	$y_A = \left[\dfrac{\tan\theta_0}{2\pi^2 j^2}\dfrac{N_{\max}^2}{f_0^2} ab^2\right]^{1/3}$	47 km
Inertial latitude scale	$L \equiv y_A/a = \left[\dfrac{\tan\theta_0}{2\pi^2 j^2}\dfrac{N_{\max}^2}{f_0^2}\dfrac{b^2}{a^2}\right]^{1/3}$	7.38×10^{-3} (0.42°)
Inertial Coriolis scale	$\beta y_A = \left[\dfrac{1}{2\pi^2 j^2 \tan^2\theta_0} f_0 N_{\max}^2 \dfrac{b^2}{a^2}\right]^{1/3}$	9.4×10^{-7} s^{-1}

(51)

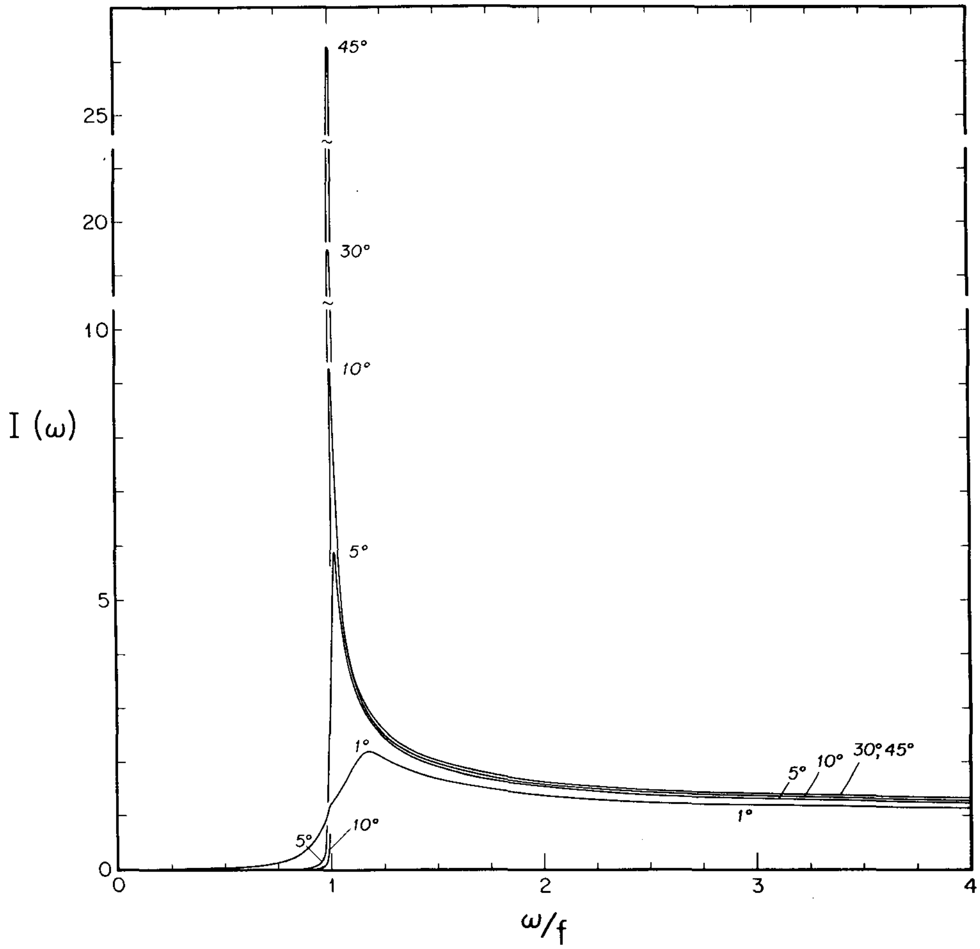

FIG. 6. As in Fig. 5 except for dv/dz. The peaks for 30° and 45° latitudes are offscale at 19.5 and 26.3. Mode weighting is by $j^2(j^2 + j_*^2)$ with an upper limit $j = 100$.

Here L is the Airy latitude scale (in radians), and βy_A in f units; βy_A is also the Airy frequency scale. Numerical values are for $b = 1$ km, $N_{\max} = 5.24 \times 10^{-3}\ \mathrm{s}^{-1}$ (3 cph), $N_0 = \frac{1}{2}N_{\max}$, $j = j_* = 3$, $\theta = 30°$, $f_0 = 7.3 \times 10^{-5}\ \mathrm{s}^{-1}$, $a = 6370$ km.

In order for the turning point approximation to be valid, the equatorial waveguide (between $-\theta_0$ and θ_0) must be wide as compared to the Airy scale L. From (51)

$$\frac{\theta_0}{L} = \frac{1}{2}\left(4\pi\frac{f_0}{N_{\max}}\frac{a}{b}j\theta_0\right)^{2/3}$$
$$= 2K_0^2 j^{2/3}\theta_0^{4/3} \approx 85 j^{2/3}\theta_0^{4/3}. \qquad (52)$$

At 5° latitude, $\theta_0/L = 3.3j^{2/3}$, and we might barely get away with the turning point approximation. The 1° latitude curve is beyond the approximation, and requires Hermite polynomials for a proper treatment (Eriksen, 1980). At high latitudes the β-approximation fails. The spheroidal wave equation is generally valid, and this is the point of view followed by Fu (1980). (See also Munk and Phillips, 1968, pp. 451–452.)

In a buoyancy waveguide of thickness Δz, the corresponding ratio is

$$\frac{b}{z_A} = \left[\frac{\sqrt{2}\pi N_0}{N_{\max}}j\right]^{2/3} \approx 2j^{2/3} \qquad (53)$$

and the approximation fails for the lowest mode numbers.

10. Buoyant versus inertial limits

Figs. 7 and 8 show the comparative energy spectra

$$F_{\mathrm{KE}}(\omega) = I_f(\omega)F(\omega), \quad F_{\mathrm{PE}}(\omega) = I_N(\omega)F(\omega), \qquad (54)$$

in relative and absolute units, respectively. In the midrange $f \ll \omega \ll N$, the spectra are given by

$$F(\omega) = \text{constant } N\omega^{-2}, \qquad (55)$$

for either kinetic or potential energy. The peak at the

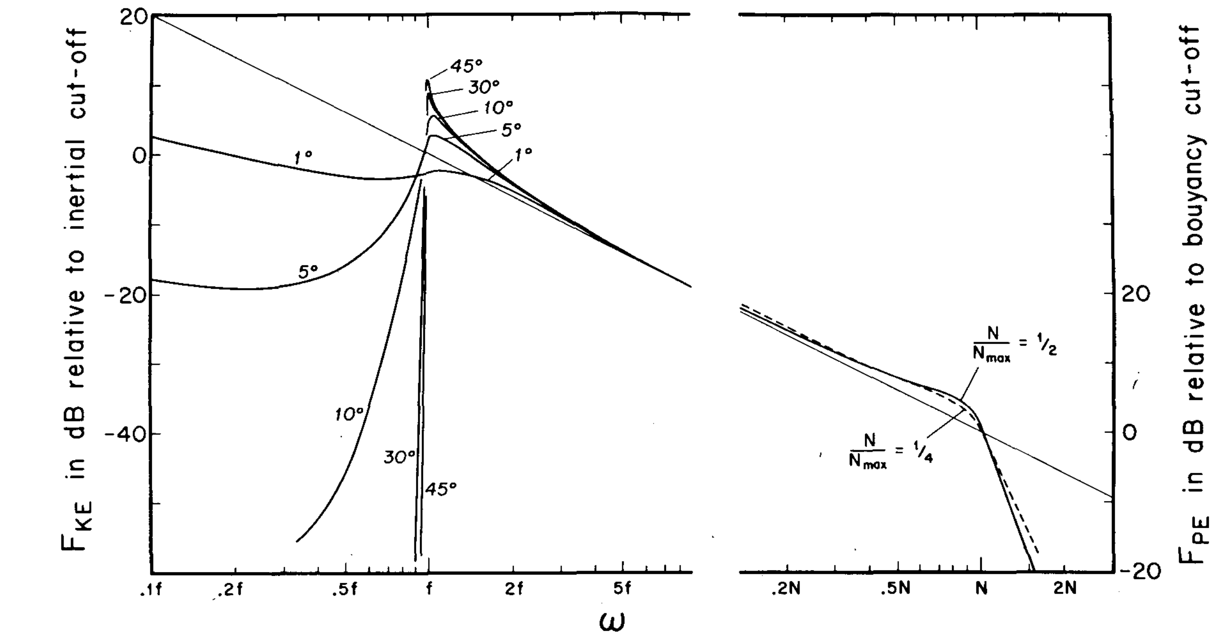

FIG. 7. Enhancement of the kinetic energy spectrum (left) and of the potential energy spectrum (right) at the inertial and buoyancy frequencies, respectively. The inertial spectrum is drawn for latitudes 1°, 5°, 10°, 30°, 45°. (At 1° latitude the turning points north and south of the equator interact, and the present treatment is no longer justified.) The buoyancy spectrum is drawn for two depths, corresponding to $N = \frac{1}{2}$ and $\frac{1}{4}$ times the maximum buoyancy frequency. The straight line corresponds to a ω^{-2} spectrum without limiting functions. The energy density is on a relative scale.

buoyancy frequency is very moderate, as has previously been found by Cairns (1975) from theory and observation. In contrast, there is a pronounced inertial peak at mid and high latitudes.

An analytical comparison is readily made by computing the amplification directly *at* the turning frequencies:

$$\begin{pmatrix} I(f) \\ I(N) \end{pmatrix} = 2\pi \begin{pmatrix} K_f \\ K_N \end{pmatrix} \mathrm{Ai}^2(0) \sum_j j^{1/3} H(j), \qquad (56)$$

with $\sum_{j=1}^{\infty} j^{1/3} H(j) = 1.79$. The amplifications are in the ratio

$$\frac{K_f}{K_N} = \left(\frac{f^2/N^2}{\beta/N'}\right)^{1/3} = \left(\frac{a 2\Omega \sin\theta \tan\theta}{bN}\right)^{1/3}. \qquad (57)$$

The ratio $bN/2\Omega \sin\theta = bN/f$ will be recognized as the Rossby radius of deformation: the peak ratio is proportional to cube root of the ratio of the earth's radius to the Rossby radius. At 30° latitude the ratio K_f/K_N is 4.7. The ratio increases toward higher latitudes, but eventually our solution is limited by the β approximation. Toward the equator the ratio diminishes as $\theta^{2/3}$.

In general, the spectra in Fig. 7 cut off sharply below the inertial frequency; an exception occurs at very low latitude, where the spectrum resumes the rise toward decreasing frequency, though at a lesser rate. This has to do with the evanescent poleward extension of low modes, prior to being exponentially cut off. We now write $\mathrm{Ai}(\eta) = \mathrm{Ai}(0) + \eta \mathrm{Ai}'(0)$ for a linear extension of the Airy function, with $\eta_m = -\mathrm{Ai}(0)/\mathrm{Ai}'(0) = +1.372$ designating the associated zero intercept. For $\eta > \eta_m$ the Airy functions are exponentially reduced. From (49) $\eta = j^{2/3} K_f^2 \phi^2(\mu)$. To derive the largest latitude (the largest K_f) for which there is a significant subinertial contribution, we set $\eta = \eta_m$ and $j = 1$. For small frequencies $\phi^3 \approx \frac{3}{2} \sin\mu$, hence $(K_f)_m{}^3 = \eta_M{}^{3/2}(\frac{3}{2} \times \sin\mu)$. From the definition (46) of K_f, the associated latitude is

$$\theta_m = \frac{\eta_m{}^{3/4}}{(\frac{3}{2}\sin\mu)^{1/2} K_0{}^{3/2}}$$
$$= 3.6°, 3.8° \quad \text{for} \quad \mu = 90°, 60°,$$

corresponding to $\omega = 0$ and $\omega = \frac{1}{2}f$, respectively. From Eq. (52), setting $\theta_0 = \theta_m$, one obtains $\theta_0/L = 2\eta_M(\frac{3}{2}\sin\mu)^{2/3} j^{2/3} \approx 2j^{2/3}$. So the approximation is poor for the lowest modes.

To obtain the asymptotic expansion, we use the low-frequency approximation $\phi^3 = 1.5$ for μ near 90°. Then from (50)

$$G(\omega,j) = 2\pi K_f \phi j^{1/3} \cos\mu [\mathrm{Ai}(0) + \eta\ \mathrm{Ai}'(0)]^2,$$
$$\eta = j^{2/3} K_f^2 \phi^2,$$

with $j = 1, 2, \ldots, j_m \approx \eta_m{}^{3/2} K_f{}^{-3} \phi^{-2}$.

The important consideration is the linear dependence on $\cos\mu = \omega/f$. Thus $\omega^{-2} I(\omega)$ is proportional

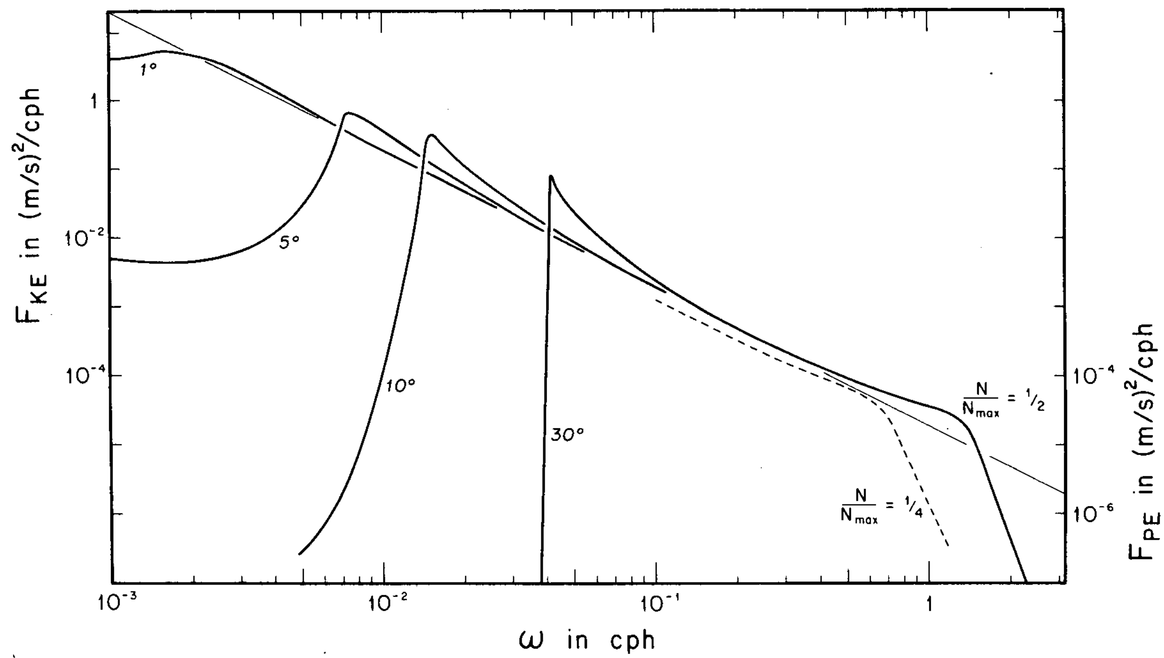

FIG. 8. As in Fig. 7 except drawn to absolute units of frequency and energy density. The solid curves are for indicated latitudes at a depth of 700 m ($N = \frac{1}{2}N_{max} = 1.5$ cph $= 2.62 \times 10^{-3}$ rad s^{-1}); the dashed curve is for a depth where $N = \frac{1}{4}N_{max}$ (~1400 m). At low frequencies the kinetic energy is plotted, at high frequencies the potential energy is plotted [1 (m s^{-1})^2 cph^{-1} corresponds to 10^3 J cph^{-1}]. At mid-frequencies (centered at ~0.25 cph) the spectrum falls off as ω^{-2} and consists of equal parts of kinetic and potential energy, independent of latitude but proportional to N.

to ω^{-1} at low frequencies and at latitudes of less than 4°, consistent with Fig. 7. But here we have gone beyond the scope of the present treatment. A discussion of equatorial behavior is given by Eriksen (1980).

11. The inertial cusp

There is now some evidence (Wunsch and Webb, 1979; Eriksen, 1980) that the energy *density* at intermediary frequencies remains independent of latitude, within narrow limits, i.e.,

$$F(\omega) \approx N\omega^{-2}, \quad f \ll \omega \ll N, \tag{58}$$

TABLE 1. Table of $\int_{x_l}^{x_u} dx\, x^{-2}\mathcal{I}(x)$ for step, GM and for Airy limiting functions at stated latitudes.

x_l to x_u		½ to 1	1 to 2	0 to 4	0 to ∞
$\int_{x_l}^{x_u} dx\, x^{-2}H(x)$		0	0.50	0.75	1
$\int_{x_l}^{x_u} dx\, x^{-2}H(x)x(x^2-1)^{-1/2}$		0	1.05	1.32	½π
$\int_{x_l}^{x_u} dx\, x^{-2}I(x)$	45°	0.19	1.58	2.09	
	30°	0.15	1.55	2.02	
	10°	0.11	1.37	1.79	
	5°	0.13	1.15	1.59	
	1°	0.20	0.52	1.44	*

* Beyond approximation.

in contrast to the *energy*-preserving GM spectrum $F(\omega) \approx f\omega^{-2}$. The spectrum including the inertial cusp is

$$I(\omega)F(\omega), \quad f \leq \omega \ll N. \tag{59}$$

The integrated energy is

$$\int_{\omega_l}^{\omega_u} d\omega I(\omega)F(\omega) = \text{constant} \int_{x_l}^{x_u} dx x^{-2}\mathcal{I}(x),$$
$$x = \omega/f. \tag{60}$$

We consider three cases for the limiting function $\mathcal{I}(x)$:

Step: $\mathcal{I}(x) = H(x)$,

GM: $\mathcal{I}(x) = H(x)x(x^2-1)^{-1/2}$,

Airy: $\mathcal{I}(x) = I(x)$; Eq. (48) for $x \geq 1$,

Eq. (50) for $x \leq 1$.

For the first two cases, the results are

$$\text{Step:} \int dx x^{-2}\mathcal{I}(x) = 1 - 1/x_u$$

$$\text{GM:} \int dx x^{-2}\mathcal{I}(x) = \cos^{-1}(1/x_u).$$

The Airy case was evaluated by numerical quadrature.

Table 1 gives some examples. The GM limiting function has twice the energy of the step limit in the inertial band $\omega = f$ to $\omega = 2f$; for the Airy limiting function the ratio is 3:1 at midlatitudes. The differences are not crucial; they could be accommodated by a corresponding change in the "universal" energy parameter.

Acknowledgments. This work has been supported by the Office of Naval Research. Carl Wunsch, Charles Eriksen, Chris Garrett and Lee-Lueng Fu have made helpful suggestions.

APPENDIX

Dispersion Scaling

This closely follows Munk and Phillips (1968). From Eqs. (16) and (51) we find

$$L = (\tfrac{1}{2} \tan\theta_0)^{1/3}(c/fa)^{2/3}. \qquad \text{(A1)}$$

The appropriate y scale is $y_A = La$. Thus $d/dy = O(La)^{-1}$. From (11) and (12)

$$k = O(La)^{-1}. \qquad \text{(A2)}$$

Let $U, V = O(L^0), p = O(L^m)$. This gives $f = kcL^m$ for either (11) or (12), or $f/kc = L(fa/c) = L^m$, and so in view of (A1) $m \geqslant -\tfrac{1}{2}$. Similarly from (10) $m \geqslant +\tfrac{1}{2}$. Thus,

$$U, V = O(1), \quad P = O(L^{1/2}) \qquad \text{(A3)}$$

and the right-hand side of either (11) or (12) is small compared to the left-hand side by a factor L.

We now compare the terms k^2 and $\beta k/\omega$ in Eq. (39). Multiply by a^2, and use $f = O(\beta a)$. From (A2), the two terms are of order L^{-2} and L^{-1}, respectively.

REFERENCES

Cairns, J. L., 1975: Internal wave measurements from a mid-water float. *J. Geophys. Res.*, **80**, 299–306.

Desaubies, Y. J. F., 1973: Internal waves near the turning point. *Geophys. Fluid Dyn.*, **5**, 143–54.

——, 1975: A linear theory of internal wave spectra and coherences near the Väisälä frequency. *J. Geophys. Res.*, **80**, 895–99.

Eriksen, C. C., 1978: Measurements and models of fine structure, internal gravity waves, and wave breaking in the deep ocean. *J. Geophys. Res.*, **83**, 2989–3009.

——, 1980: Evidence for a continuous spectrum of equatorial waves in the Indian Ocean. *J. Geophys. Res.*, **85**, 3285–3303.

Fu, L.-L., 1980: Observations and models of inertial waves in the deep ocean. Ph.D. dissertation, MIT/WHOI Joint Program in Oceanography, 91 pp.

Garrett, C. J. R., and W. H. Munk, 1972: Space-time scales of internal waves. *Geophys. Fluid Dyn.*, **2**, 225–64.

Munk, W. H., 1980: Internal wave and small scale processes. *The Ocean Environment*, C. Wunsch and B. Warren, Eds., The MIT Press, 264–291.

——, and N. Phillips, 1968: Coherence and band-structure of inertial motion in the sea. *Rev. Geophys.*, **6**, 447–72.

Wunsch, C., and D. Webb, 1979: The climatology of deep ocean internal waves. *J. Phys. Oceanogr.*, **9**, 235–43.